Materials Science-Poland, 34(4), 2016, pp. 863-867
http://www.materialsscience.pwr.wroc.pl/
DOI: 10.1515/msp-2016-0108

DE GRUYTER OPEN

AFM studies of pits formation on KBr(1 0 0) during its dissolution by water*

JUSTYNA PERS†, BOGDAN BARWIŃSKI, MIŁOSZ GRODZICKI, ANTONI CISZEWSKI

Institute of Experimental Physics, University of Wroclaw, pl. Maxa Borna 9, 50–204 Wroclaw, Poland

The formation of etch pits along screw dislocations on KBr(1 0 0) surface during its dissolution by water is investigated by means of atomic force microscopy (AFM). Clean KBr(1 0 0) is obtained by cleavage. A weak solution of water in isopropyl alcohol is used to investigate the etching in real time. Observations of the etch pit evolution with etching time show that concentration of atomic steps on the pit walls and dissolution rate of the walls vary up to complete dissolution of the screw dislocation. The screw dislocation removal stabilizes the dissolution, resulting in constant values of atomic steps concentration on the pit walls and their dissolution rate during further etching, which continues according to the crystal dissolution stepwave model. It was found that the movement of AFM scanning tip essentially affected the etching process.

Keywords: *dissolution; stepwave model; screw dislocation; KBr; AFM*

1. Introduction

The solid-state dissolution processes are a subject of continuous research attempts whose results are of interest both for basic knowledge and for applications. Gained data extend the knowledge about fundamental processes of environmental geology and engineering. Acquired knowledge is widely applied in different areas of industry where passivation, corrosion or ablation are involved.

Conventional methods employed in the solid-state dissolution investigations, which are based on measurements of instantaneous ion concentration changes of the solution, do not yield direct information about the influence of surface structure and topography on the kinetics of the process. The results of averaging do not uncover the entire run of dissolution, and elucidation of the mechanism for a given area of the phase boundary is not possible [1, 2]. A breakthrough in this field has been made with the advent of experimental works employing atomic force microscopy (AFM) [3, 4]. The technique enables visualization of microscopic events associated with the solid-state dissolution in situ. Moreover, changes in topography of a surface can be observed in the real time, provided that they occur with a rate comparable to that of imaging by the microscope [5, 6].

From the AFM investigations, various models of crystal dissolution mechanism [7, 8] have been derived, which are generally based on the Burton-Cabrera-Frank (BCF) theory [9–11]. Currently, theoretical models enable description of the dissolution process for a wide group of minerals [12–21].

Herein, the results of our studies on etch pits formation during dissolution of the ⟨1 0 0⟩ oriented single KBr crystal are reported. According to our best knowledge these are the first direct observations of water dissolution of KBr(1 0 0) face which have been carried out in real time. As a material, KBr is soft (1.5 Mohs hardness) with density of 2.74 g cm^{-3} and relatively high melting point (748 °C). Owning NaCl structure it can be easily cleaved along the {1 0 0} planes. Well water soluble at room temperature it is practically insoluble in alcohol. For the investigation, a solution of small amount of water with isopropyl alcohol was used. Water concentration in the solution has been

*Thie paper was presented at XIII Seminar on Surfaces and Thin-Film-Structures, Szklarska Poręba, Poland, 2015.

†E-mail: jpers@ifd.uni.wroc.pl

chosen so low in order to reduce KBr dissolution rate to a level allowing the real time AFM observations of etch pits formation.

It was found that at screw dislocations, dissolution results in creation of pyramid-like pits. The formation process of the pits at defect sites and their evolution up to the moment of dissolution stabilization due to complete removal of the screw dislocation by the etching are discussed. Further, dissolution mechanism is explained in terms of the stepwave model.

2. Experimental

The AFM apparatus (Nanoscope III, Digital Instruments; Veeco) with a liquid cell was used for investigations performed at room temperature. Surface imaging was made in contact mode. Scanner could image a surface area of 13 × 13 μm^2 and 9 × 9 μm^2 in air and liquid, respectively. An AFM probe was applied with a cantilever 200 μm long and 0.06 $N \cdot m^{-1}$ elastic constant, and a tip of 2.86 μm height, 4 μm base diameter and 10 nm radius (NP-S10, Veeco). The clean (1 0 0) surface of the crystal was obtained by cleaving, which was followed by AFM examination in air. Then, the preparation was placed in the liquid cell containing pure isopropyl alcohol solvent in order to choose optimum scanning conditions. Scanning frequency was about 0.5 Hz, and scanning period 3 minutes. Afterward, H_2O was introduced with a pipette to have a 0.2 % solution.

The solution was passed through the liquid cell with a rate of 0.05 $mL \cdot min^{-1}$. The flow rate was adjusted with commercial valves. In such conditions, the crystal water dissolution and the KBr(1 0 0) surface etching process was investigated. Circulation of the solution did not affect the tip-surface contact. AFM image analysis was performed using the WSxM program [22].

3. Results and discussion

The AFM measurement on the KBr(1 0 0) surface, which was made just after cleaving the crystal, unveiled terraces of the width between 0.1 and 2 μm, with a majority of ∼1 μm ones. Their height is 0.33 nm, which corresponds to half the lattice parameter (1/2 a) of KBr. Thus, the surface is smooth and alternately decorated with K^+ and Br^- ions. A number of defects appeared, such as screw and edge dislocations, and KBr voids (Fig. 1a). We focused our attention on crystal dissolution progress in the site of a left-handed screw dislocation (Fig. 1b). It was of helix type with three coils and a base diameter of about 5 μm. The width of helical terraces ranged from 0.5 to 1.5 μm. The magnitude of Burgers vector for the dislocation was 1/2 a.

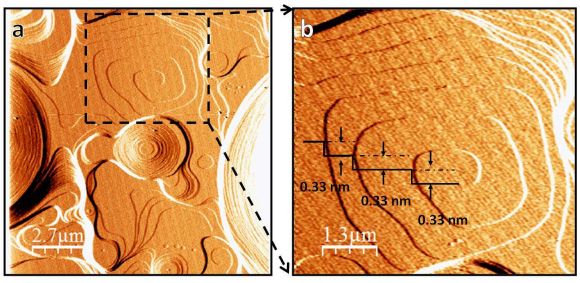

Fig. 1. (a) Horizontal derivatives of a KBr(1 0 0) surface just after crystal cleaving; AFM in-the-air imaging, (b) the area of the square 6.1 × 6.1 μm^2 marked with the dashed line in (a).

Treating the sample with the solvent allowed the optimum AFM operation and a stable working mode during recording of the KBr dissolution process. The isopropyl alcohol caused a slight deterioration of image quality with disappearance of terrace edges. Deterioration of the resolution in the direction normal to the surface was not due to dissolution of material because repeated scanning of the same surface area exposed to isopropanol did not affect the sample's topography. Nonetheless, the shape of voids changed from that of a round object to the one with perpendicular walls and sides parallel to the ⟨1 1 0⟩ directions. Roughness coefficient (RMS, Rq-Root Mean Square) for an area of 9 × 9 μm^2 was found to be 3.5 nm.

In order to slow down the dissolution, a weak isopropanol solution of water was applied and the liquid was passed with a steady rate through the liquid cell. The measurements were done for

the solution of water concentration equal to 0.2 %. For the area 9 × 9 μm^2, the RMS roughness after 4 and 150 minutes was 3.6 and 7.8 nm, respectively. The rise in the factor must have been connected with etching leading to the appearance of numerous cavities in the dislocation sites.

The evolution of etch pits in the screw dislocation sites has been analyzed in detail: an example is shown in Fig. 1b. The etch pit has a square-base pyramid shape whose axis is perpendicular to the sample surface. The base area increases with duration of the exposure to water (Fig. 2). Sides of the base are parallel to the ⟨1 1 0⟩ directions. In order to estimate the relative rate of the pit's volume etching, an analysis of its size and form vs. time has been made. Exemplary profiles of the pit evolution along [0 1 0] and [1 $\underline{1}$ 0] directions are shown in Fig. 3. Dashed lines mark the 10 nm long segment of the pit depth, which serves as the reference region for which the changes in the slope of the pit walls are measured. The angle of inclination along the [1 0 0] direction gradually increases up to 135 minutes of dissolving to obtain a constant value after this time.

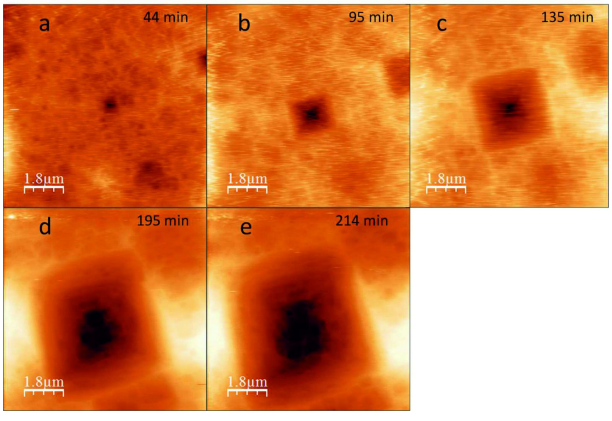

Fig. 2. Evolution of the etch pit versus exposure to a weak isopropanol solution of water. Exposure time in minutes is given in the upper right corner of each image. Area of scan is 9.0 × 9.0 μm^2. Z scales of images (a-e) are described from dark (0 nm) to light 38, 39, 32, 36 and 25 nm, respectively.

Examination of the measurement data acquired from different crystallographic directions (Fig. 4)

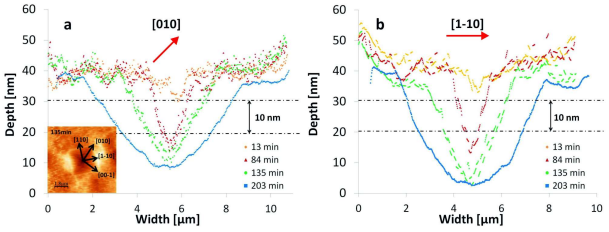

Fig. 3. Hollow profiles along directions (a) [0 1 0] and (b) [1 $\underline{1}$ 0] for various times of exposure to the solution. Inset in (a) shows crystallographic directions of the hollow.

shows that the rise in the hole diameter gradually proceeds to accelerate after 84 minutes. The effect is caused by the fact that at the early etching stage an excess material in the vicinity of the hole must be removed first. Up to this moment, the etching rate along the screw dislocation is fixed and amounts to 0.5 × 10^{-2} nm·s^{-1} (as is marked in Fig. 4a). After 84 minutes of dissolution, the rate has no longer its linear character and begins to differ for different directions. For ⟨1 1 0⟩ and ⟨1 0 0⟩ directions, the diameter rise rates are 6.5 × 10^{-4} μm·s^{-1} and 5.6 × 10^{-4} μm·s^{-1}, respectively. Removal of the excess material from the surface ensures an easy movement of atomic steps and lowers the step density of the hollow walls, which leads to a higher spacing between the steps. The hollow's walls are spreading like a wave on a smooth surface of water after dropping in a small stone. After 135 minutes of dissolution the screw dislocation dissolves completely. From this moment dissolution process begins to flatten the pit. Changes in the base side length of the pit are illustrated in Fig. 4b. Transformation of the base shape of the pit from square to rectangular shape indicates that removal of material from the ⟨1 0 0⟩ directions is slower due to a relatively high atomic packing density along these directions. Both the change of the shape and the constant pit-wall dissolution rate, observed after 135 minutes of water etching, are caused by the dissolution of the screw dislocation, which acts as a generator of atomic steps. Generation of atomic steps by the dislocation promotes the etching. Lack of this source stabilizes the dissolution process.

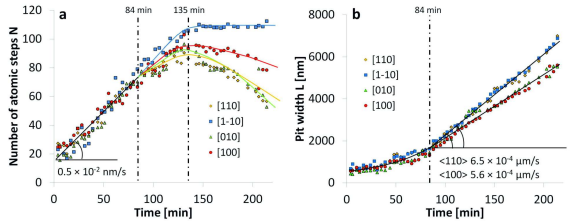

Fig. 4. (a) Number of atomic steps and (b) base side width of the etched hollow as a function of time along ⟨1 1 0⟩ and ⟨1 0 0⟩ directions.

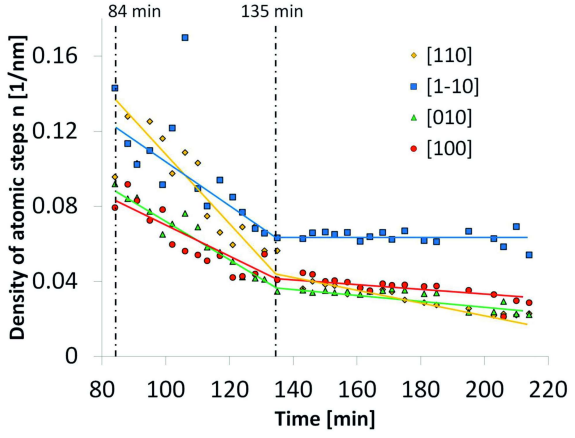

Fig. 5. Density of atomic steps as a function of time along ⟨1 1 0⟩ and ⟨1 0 0⟩ directions.

The observed here etching phenomenon is in accord with the relatively new dissolution model of advancing wave of Lasaga and Lüttge [23]. In terms of their (so called stepwave) model, screw dislocation should be interpreted as a generator of atomic steps. Pit etching is a result of the removal of material that creates atomic steps. It causes their migration away from the center leading to total dissolution of the crystal [24]. Our observations of the process indicate that, among others, the spacing between the steps increases with increasing distance from the axis of the etched pit, which is in accord with the model. Similar processes have previously been observed [25–33].

Moreover, we have found that the AFM probe affects the dissolution process during scanning the sample surface under conditions of a steady flow of the solution. The 3D tip of the cantilever disturbs the flow of the liquid and so the dissolved mass transfer, which was earlier reported [34, 35]. Local changes in crystallographic orientation and liquid flow lead to lowering of the efficiency of material removal. The high concentration of the dissolved substance over the sample surface locally saturates the solution, which inhibits the dissolution run. A scanning sweep of the tip gathers the dissolved material, which leads to the appearance of build-ups. The profile in the [1 1̲ 0] direction deviates from the trapezoid, see black line in Fig. 6. Material gathered by the tip is accumulated between the bottom and the walls of the hollow. Data that produce the surface topography image are acquired in two directions of cantilever motion: the probe is displaced along the first scanning line (to the left) and backward. A large accumulation of the swept material occurs on the right-hand side of the profile [1 1̲ 0]. The effect is lacking for the [1 1 0] direction.

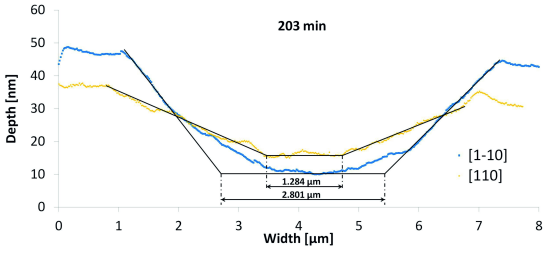

Fig. 6. Influence of tip scanning on the shape of a hollow. Profiles along [1 1 0] and [1 1̲ 0] directions were observed in 203 minutes of exposure to the solution.

4. Conclusions

The presented results concern the process that occurs at the phase boundary between the KBr(1 0 0) surface and a weak isopropanol solution of water. The alcohol solvent does not cause any dissolution of the KBr crystal surface. A small amount of water added to the alcohol initiates the dissolution process. In the sites of screw dislocations on the (1 0 0) surface, a rise in dissolution rate is observed, which leads to etch pits formation. The pits are of a square base pyramid form. Time dependence of the pits growth enables estimation of the relative dissolution rate in the dislocation site. Distance between the atomic

steps on the walls of the pit saturates after the screw dislocation dissolution. The pit walls spread outward with a constant rate. Kinetics of the pit evolution can be explained in terms of the stepwave model. A clear effect of AFM probe on the surface dissolution process is observed. The scanning itself disturbs the liquid flow and transfer of the dissolved material.

Acknowledgements

The University of Wroclaw under 1471/M/IFD/11 and 2458/M/IFD/14 grants supported this work. The authors thank Dr. Stanisław Surma for helpful discussions and his assistance during preparation of the manuscript.

References

[1] Brantley S.L., Crane S.R., Crerar D.A., Hellmann R., Stallard R., *Am. Chem. Soc.*, 323 (1986), 635.
[2] Lasaga A.C., Blum A.C., *Geochim. Cosmochim. Acta*, 50 (1986), 2363.
[3] Hillner P.E., Gratz A.J., Manne S., Hansma P.K., *Geology*, 20 (1992), 359.
[4] Gratz A.J., Manne S., Hansma P.K., *Science*, 251 (1991),1343.
[5] Binning G., Quate C.F., Gerber CH., *Phys. Rev. Lett.*, 56 (1986), 930.
[6] Dove P.M., Platt F.M., *Chem. Geol.*, 127 (1996), 331.
[7] Dove P.M., Nizhou H., de Yoreo J.J., *PANS*, 102 (2005), 15357.
[8] Snyder R.C., Doherty M.F., *AIChE Journal*, 53 (2007), 1337.
[9] Burton W.K., Cabrera N., Frank F.C., *Nature*, 163 (1949), 398.
[10] Burton W.K., Cabrera N., Frank F.C., *Philos. Trans. Royal. Soc. Lond. A. Match. Phys. Sci.*, 243 (1951), 299.
[11] Cabrera N., Levine M.M., *Philos. Mag.*, 1 (1956), 450.
[12] Lüttge A., Winkler U., Lasaga A.C., *Geochim. Cosmochim. Acta*, 67 (2003) 1099.
[13] Advirson R.S., Ertan I.E., Amonette J.E., Lüttge A., *Geochim. Cosmochim. Acta*, 67 (2003), 1623.
[14] Asta M.P., Cama J., Soler J.M., Arvidson R.S., Lüttge A., *Am. Miner.*, 93 (2008), 508.
[15] Kurganskaya I., Arvidson R.S., Fischer C., Lüttge A., *Geochim. Cosmochim. Acta*, 97 (2012), 120.
[16] Xiao Y., Lasaga A.C., *Geochim. Cosmochi. Acta*, 58 (1994), 5379.
[17] Risthaus P., Bosbach D., Becker U., Putnis A., *Physicochem. Eng. Aspects*, 191 (2001), 201.
[18] Ichikawa K., Sato S., Shimomura N., *Pure Appl. Chem.*, 76 (2004), 115.
[19] MacPherson J.V., Unwin P.R., Hillier A.C., Bard A.J., *J. Am. Chem. Soc.*, 118 (1996), 6445.
[20] Vavouraki I.A., Putnis CHR.V., Putnis A., Koutsoukos P.G., *Crys. Growth Des.*, 10 (2010), 60.
[21] Oelkers E.H., *Geochim. Cosmochim. Acta*, 65 (2001), 3671.
[22] Horcas I., Fernández R., Gómez-Rodríguez J.M., Colchero J., Gómez-Herrero J., Baro A.M., *Rev. Sci. Instrum.*, 78 (2007), 013705.
[23] Lasaga A.C., Lüttge A., *Science*, 291 (2001), 2400.
[24] Lasaga A.C., Lüttge A., *Eur. J. Mineral.*, 15 (2003), 603.
[25] Zahng L., Lüttge A., *J. Phys. Chem. B*, 112 (2008), 1736.
[26] Zahng L., Lüttge A., *Geochim. Cosmochim. Acta*, 73 (2009), 6757.
[27] Zahng L., Lüttge A., *Geochim. Cosmochim. Acta*, 73 (2009) 2832.
[28] Casey W.H., Carr M.J., Graham R.A., *Geochim. Cosmochim. Acta*, 52 (1988), 1545.
[29] Schott J., Brantley S.L., Crerar D.A., Guy C., Borcsik M., Willaime C., *Geochim. Cosmochim. Acta*, 53 (1989), 373.
[30] Blum A.E., Yund R.A., Lasaga A.C., *Geochim. Cosmochim. Acta*, 54 (1990), 283.
[31] Vinson M., Lüttge A., *Am. J. Sci.*, 305 (2005), 119.
[32] Fewless A.T., Zhang L., Lüttge A., *Geochim. Cosmochim. Acta*, 69 (2005), A779.
[33] Cama J., Zhang L., de Giudici G., Soler J.M., *Geochim. Cosmochim. Acta*, 74 (2010), 4298.
[34] Gasperino D., Yeckel A., Olmsted B.K., Ward M.D., Derby J.J., *Langmuir*, 22 (2006), 6578.
[35] Burt D.P., Wilson R.N., Janus U., MacPherson J.V., Unwin P.R., *Langmuir*, 24 (2008), 12867.

Received 2016-04-20
Accepted 2016-09-23